⌘ *Author's Choice*

THE JOURNAL OF BIOLOGICAL CHEMISTRY VOL. 285, NO. 28, pp. 21817–21823, July 9, 2010

Disruption of Lysosome Function Promotes Tumor Growth and Metastasis in *Drosophila**[S]

Received for publication, April 7, 2010, and in revised form, April 22, 2010 Published, JBC Papers in Press, April 25, 2010, DOI 10.1074/jbc.M110.131714

Congwu Chi[‡1], Huanhu Zhu[‡1], Min Han[‡§2], Yuan Zhuang[‡¶], Xiaohui Wu[‡3], and Tian Xu[‡‖2,4]

From the [‡]Institute of Developmental Biology and Molecular Medicine, Fudan-Yale Center for Biomedical Research, School of Life Science, Fudan University, Shanghai 200433, China, the [§]Howard Hughes Medical Institute, Department of Molecular, Cellular, and Developmental Biology, University of Colorado, Boulder, Colorado 80309-0347, the [¶]Department of Immunology, Duke University Medical Center, Durham, North Carolina 27701, and the [‖]Howard Hughes Medical Institute, Department of Genetics, Yale University School of Medicine, New Haven, Connecticut 06536

Lysosome function is essential to many physiological processes. It has been suggested that deregulation of lysosome function could contribute to cancer. Through a genetic screen in *Drosophila*, we have discovered that mutations disrupting lysosomal degradation pathway components contribute to tumor development and progression. Loss-of-function mutations in the Class C vacuolar protein sorting (VPS) gene, *deep orange* (*dor*), dramatically promote tumor overgrowth and invasion of the Ras^{V12} cells. Knocking down either of the two other components of the Class C VPS complex, *carnation* (*car*) and *vps16A*, also renders Ras^{V12} cells capable for uncontrolled growth and metastatic behavior. Finally, chemical disruption of the lysosomal function by feeding animals with antimalarial drugs, chloroquine or monensin, leads to malignant tumor growth of the Ras^{V12} cells. Taken together, our data provide evidence for a causative role of lysosome dysfunction in tumor growth and invasion and indicate that members of the Class C VPS complex behave as tumor suppressors.

The lysosome plays important roles in many physiological processes and pathological conditions. It has been suggested that deregulation of lysosome function could contribute to tumor development. For example, altered trafficking of lysosomal cathepsins has been found in cultured cancer cells and in malignant tumors in patients (1–3). However, evidence that lysosome dysfunction plays a causative role in tumor development and progression remains elusive.

Proteins responsible for lysosomal delivery and degradation are highly conserved among different eukaryotic species. For example, genetic screens in yeast have identified a group of genes encoding the Class C vacuolar protein sorting (VPS)[5] complex, which is involved in the docking and membrane fusion of endosomal vesicles and the lysosome-like yeast vacuole. Mutations in Class C VPS complex genes cause similar phenotypes characterized as accumulation of enlarged multivesicular bodies and defects in sorting cargoes to the vacuole (4, 5). In *Drosophila*, studies have shown that the components of the Class C VPS complex, *e.g.* Deep orange (Dor), Carnation (Car), and Vps16A, play a similar role, as do their yeast homologues (6, 7). The *Drosophila* lysosomal delivery system is also found to be involved in the development of eye pigmentation. Mutations in *car* and *dor* cause severe defects in intracellular trafficking to the lysosome and defects in eye color (8). The Class C VPS complex has been shown to be functionally conserved from flies to human (9–15).

To identify genes involved in tumor progression, we have performed a genetic screen for mutations on the X chromosome utilizing a recently established *Drosophila* metastasis model (16). In the developing eye epithelium, GFP-labeled clones of cells are simultaneously expressing the oncogenic *Ras* (Ras^{V12}) protein and are homozygous for newly induced X-linked mutations. Because clones of Ras^{V12} cells exhibit benign overgrowth, the metastatic phenotype can be easily visualized by the invasion of GFP-positive cells from the primary tumor to other tissues. Here we report the identification of *dor*, a homologue of yeast *vps18*, in the screen and uncovered the causative role of lysosomal dysfunction in tumor progression and metastasis by analyses with both mutations and antimalarial drugs.

EXPERIMENTAL PROCEDURES

Fly Strains and Genetics—Flies were raised at 25 °C on standard medium. Duplication and deficiency lines used in mutation mapping were obtained from the Bloomington Stock Center and Kyoto Stock Center. dor^{C107} and dor^{D185} were isolated from an ethyl methanesulfonate mutagenesis screen, whereas dor^{8} was obtained from the Bloomington Stock Cen-

* This work was supported by National Natural Science Foundation of China (Grant 30270694), Chinese Key Projects for Basic Research (973) (Grant 2006CB806702), Hi-tech Research and Development Project (863) (Grant 2007AA022101), 211 and 985 projects of Chinese Ministry of Education, Shanghai Pujiang Program (Grant 05PJ14024), and Shanghai Rising-Star Program (Grant 06QA14006). This work was also supported in part by National Institutes of Health NCI Grant R01 CA069408 (to T. X.).

⌘ *Author's Choice*—Final version full access.

[S] The on-line version of this article (available at http://www.jbc.org) contains supplemental Fig. 1.

[1] Both authors contributed equally to this work.

[2] Howard Hughes Medical Institute Investigators.

[3] To whom correspondence may be addressed. Tel.: 86-21-65643718-202; Fax: 86-21-65643770; E-mail: xiaohui_wu@fudan.edu.cn.

[4] To whom correspondence may be addressed: Howard Hughes Medical Institute, Dept. of Genetics, Yale University School of Medicine, 295 Congress Ave., New Haven, CT 06536. Tel.: 203-737-2623; Fax: 203-737-1762; E-mail: tian.xu@yale.edu.

[5] The abbreviations used are: VPS, vacuolar protein sorting; GFP, green fluorescent protein; RFP, red fluorescent protein; RNAi, RNA interference; VNC, ventral nerve cord; AEL, after egg laying; JNK, c-Jun N-terminal kinase; WT, wild type.

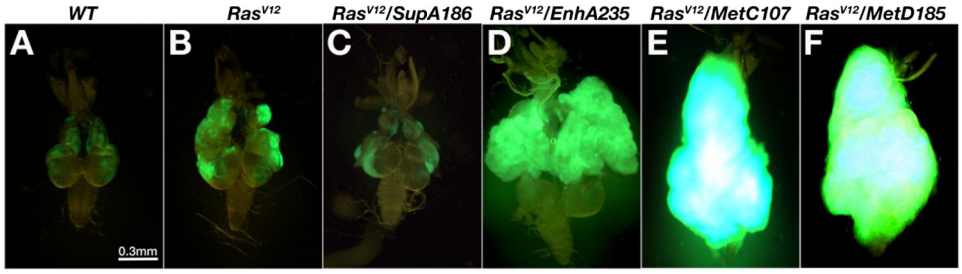

	No effect	Suppressor	Enhancer	Metastasis
No. screened:	2229 (71.5%)	516 (16.5%)	351 (11.3%)	23 (0.7%)

FIGURE 1. **Genetic screen identified mutations that promote tumor growth and metastasis of *Ras^{V12}* cells.** *A–F*, dorsal views of dissected cephalic complexes from third-instar larvae of mentioned genotypes are shown. The anterior is to the *top* in all panels; the mouth hook is to the *top*, and the VNC is pointing down in all panels. *ey-FLP*-introduced homozygous clones are labeled by GFP (*green*). The summary of the screen was shown at the *bottom*. Mutants are grouped into four subcategories based on their tumor progression phenotypes. The screen results are listed as the number of mutant lines and its percentage in each subcategory.

ter. The DNA fragment for inverted repeats in the *car^{RNAi}* construct was generated by PCR and cloned into pWIZ (17). The transgenic flies were established using standard procedures (18). *UAS-dor*, *vps16A^{RNAi}*, and *UAS-GFP-LAMP* strains were gifts from Helmut Krämer. The *UAS-atg5^{RNAi}* and *UAS-atg7^{RNAi}* strains were kindly provided by Thomas P. Neufeld.

Fluorescence-labeled non-invasive and invasive tumor clones were produced using *w, Tub-Gal80, FRT19A*; *ey-FLP5, Act5C>y+>Gal4, UAS-GFP* (19A GFP tester) or *w, Tub-Gal80, FRT19A*; *ey-FLP5, G454/CyO*; *Act5C>y+>Gal4, UAS-SrcRFP/TM6B*. Clones homozygous for *dor* mutations were generated from *dor* heterozygous flies by crossing with 19A GFP testers.

The genotypes for the animals described in this study are listed below. In Figs. 1*A*, 2*C*, 2*D*, *and 3B*, *w, sn^3, FRT19A/w, Tub-Gal80, FRT19A*; *ey-FLP5, Act5C>y+>Gal4, UAS-GFP/+*. In Figs. 1*B*, 3*D*, 3*E*, and 4, *I–L*, *w, sn^3, FRT19A/w, Tub-Gal80, FRT19A*; *ey-FLP5, Act5C>y+>Gal4, UAS-GFP/UAS-Ras^{V12}*. In Fig. 1*C*, *SupA186*, *w, sn^3, FRT19A/w, Tub-Gal80, FRT19A*; *ey-FLP5, Act5C>y+>Gal4, UAS-GFP/UAS-Ras^{V12}*. In Fig. 1*D*, *EnhA235*, *w, sn^3, FRT19A/w, Tub-Gal80, FRT19A*; *ey-FLP5, Act5C>y+>Gal4, UAS-GFP/UAS-Ras^{V12}*. In Fig. 1*E*, *dor^{C107}*, *w, sn^3, FRT19A/w, Tub-Gal80, FRT19A*; *ey-FLP5, Act5C>y+>Gal4, UAS-GFP/UAS-Ras^{V12}*. In Fig. 1*F*, *dor^{D185}*, *w, sn^3, FRT19A/w, Tub-Gal80, FRT19A*; *ey-FLP5, Act5C>y+>Gal4, UAS-GFP/UAS-Ras^{V12}*. In Fig. 2, *E* and *F*, *dor^{C107}*, *w, sn^3, FRT19A/w, Tub-Gal80, FRT19A*; *ey-FLP5, Act5C>y+>Gal4, UAS-GFP/+*. In Fig. 2*G*, *dor^8*, *FRT19A/w, Tub-Gal80, FRT19A*; *ey-FLP5, Act5C>y+>Gal4, UAS-GFP/UAS-Ras^{V12}*. In Fig. 2*H*, *dor^8*, *FRT19A/w, Tub-Gal80, FRT19A*; *ey-FLP5, Act5C>y+>Gal4, UAS-GFP/UAS-Ras^{V12}*; *UAS-dor/+*. In Fig. 2*I*, *dor^8*. In Fig. 2*J*, *dor^8/Y*; *Act-Gal4/+*; *UAS-dor/+*. In Fig. 3*A* (WT)), *w^{1118}*; *Act-Gal4/+*. In Fig. 3*A* (*car^{RNAi}*), *w^{1118}*; *Act-Gal4/+*; *car^{RNAi}/+*. In Fig. 3*C*, *w, sn^3, FRT19A/w, Tub-Gal80, FRT19A*; *ey-FLP5, Act5C>y+>Gal4, UAS-GFP/+*; *car^{RNAi}/+*. In Fig. 3, *F* and *G*, *w, sn^3, FRT19A/w, Tub-Gal80, FRT19A*; *ey-FLP5, Act5C>y+>Gal4, UAS-GFP/UAS-Ras^{V12}*; *car^{RNAi}/+*. In Fig. 3, *H* and *I*, *w, sn^3, FRT19A/w, Tub-Gal80, FRT19A*; *ey-FLP5, Act5C>y+>Gal4, UAS-GFP/UAS-Ras^{V12}, vps16A^{RNAi}*. In Fig. 4, *A–D*, *w, sn^3, FRT19A/w, Tub-Gal80, FRT19A*; *ey-FLP5, G454/UAS-Ras^{V12}, UAS-GFP-LAMP*; *Act5C>y+>Gal4, UAS-SrcRFP/+*. In Fig. 4, *E–H*, *dor^8, FRT19A/w, Tub-Gal80, FRT19A*; *ey-FLP5, G454/UAS-Ras^{V12}, UAS-GFP-LAMP*; *Act5C>y+>Gal4, UAS-SrcRFP/+*.

Metastasis Assays—Assays to detect metastatic behaviors were performed as described previously (16). Briefly, cephalic complexes of wandering third-instar larvae were dissected in phosphate-buffered saline, and the distribution patterns of GFP clones were carefully examined in eye-antennal discs, optical lobes, ventral nerve cords (VNCs), guts, and tracheae. The invasions of GFP clones from their original sites (eye-antennal discs and optical lobes) to VNCs (as well as guts and tracheae) were considered as metastasis events. Metastasis was considered suppressed if no metastasis event was observed or if the majority of animals pupated. All images were captured under Leica MZFLIII microscope.

Chloroquine and Monensin Feeding Assays—10% phosphate-buffered saline and ethanol were used to dissolve chloroquine (Sigma) and monensin (Sigma), respectively. In drug treatment experiments, a single drug solution was mixed into standard fly medium with a final concentration of 1 mg/ml (chloroquine) or 600 μM (monensin). Control medium for each drug was prepared by mixing standard medium with the solvent only. Crosses of parental flies were set up 1 day before they were transferred into vials for drug treatment. The third-instar larvae of the next generation were gathered for the subsequential metastasis assays.

RESULTS

A Genetic Screen for X-linked Mutations That Promote Tumor Overgrowth and Metastasis of Ras^{V12} Cells—The *Drosophila* X chromosome contains over 13% of the genome and more than 2,200 genes. However, only less than 750 X-linked genes have been phenotypically characterized. This is largely due to the difficulty in establishing lines harboring X-linked lethal mutations, which can only be stocked in females. We have established 3,119 lines with individual ethyl methanesulfonate-mutagenized X chromosomes and discovered that 1,092 lines carry recessive lethal mutations, whereas 78 of the viable lines exhibit visible morphological defects.[6] We then examined all of the mutagenized X chromosomes for their ability to promote tumor growth and invasion in cooperation with *Ras^{V12}*. As reported previously, clones of cells expressing *Ras^{V12}* in the developing eye exhibit moderate benign overgrowth and never invade into the nearby VNC or other tissues (Fig. 1, *A* and *B*). When clones of *Ras^{V12}*-expressing cells are also homozygous for a mutation in the metastasis suppressor gene, *stardust* (*sdt*), they developed into aggressive tumors with dramatic overgrowth

[6] C. Chi, H. Zhu, and T. Xu, unpublished data.

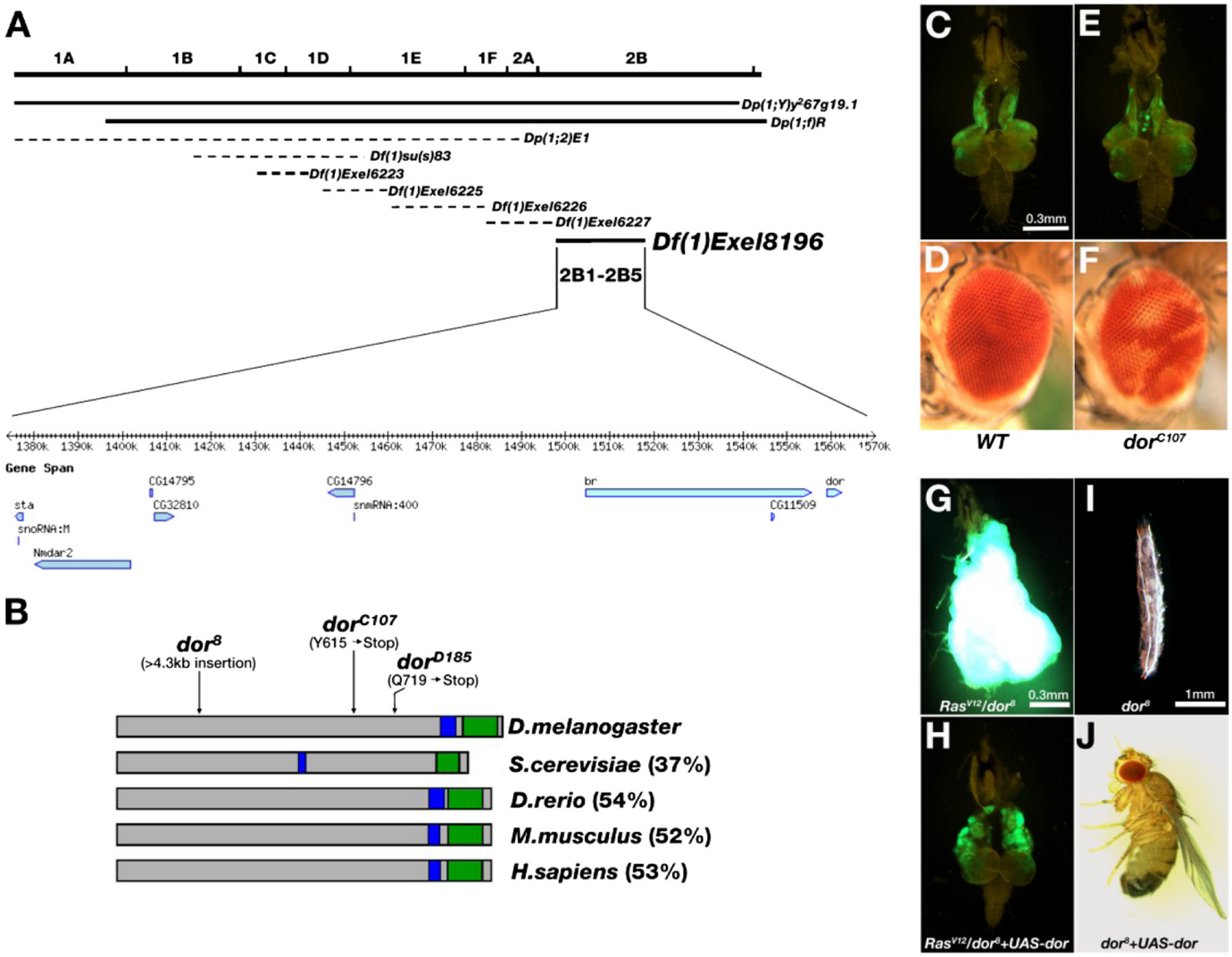

FIGURE 2. ***deep orange* behaves as a metastasis suppressor.** *A*, genetic mapping using a series of duplication and deficiency lines located the *dor*^{C107} mutation in the chromosome region of 2B1-2B5. *Solid lines* indicate the duplications and deficiencies that rescued or failed to complement with the mutation, respectively. *Dotted lines* indicate the duplications or deficiencies that failed to rescue or were able to complement the mutation, respectively. The candidate genes located within this region are shown. *B*, illustration of the Dor protein and its homologues in several species. The coiled-coil domain and the RING-H2 domain are indicated by *blue* and *green boxes*, respectively. The percentages of overall similarity between Dor and its homologues are indicated. The molecular lesions of the three *dor* alleles are also indicated. *D.melanogaster*, *Drosophila melanogaster*; *S.cerevisiae*, *Saccharomyces cerevisiae*; *D.rerio*, *Danio rerio*; *M.musculus*, *Mus musculus*; *H.sapiens*, *Homo sapiens*. *C*, *E*, *G*, and *H*, fluorescence images of dissected cephalic complexes showing GFP-labeled homozygous cell clones of indicated relevant genotypes. *D* and *F*, micrographs of mosaic compound eyes containing homozygous WT (*D*) or *dor*^{C107} (*F*) clones labeled by the *w* mutation. *I* and *J*, microscopy images of the three-instar larva (*I*) and the adult fly (*J*) with indicated genotypes. Clones homozygous for *dor*^{C107} (*E*) do not exhibit any growth advantage when compared with WT (*C*). Note the severe pigmentation loss in *dor*^{C107} clones (*F*) when compared with WT (*D*). *G–J*, the expression of full-length wild type *dor* cDNA can fully rescue *dor*^{8}-caused phenotypes. The excess growth and metastasis of *Ras*^{V12}/*dor*^{8} tumors (*G*) are completely blocked by specific expression of *UAS-dor* in these tumor clones (*H*). The image of a viable adult fly indicates that the lethality of *dor*^{8} allele (*I*) is rescued by ubiquitous expression of *UAS-dor* (*J*). *C* and *E* are in the same magnification. *G* and *H* are in the same magnification.

and invasion into VNC (16). When the newly induced X-linked mutations were examined in a similar fashion, 71.5% (2,229) of the mutations did not affect the *Ras*^{V12} phenotype (Fig. 1). 16.5% (516) of the mutations suppressed *Ras*^{V12}-induced benign overgrowth (Fig. 1*C*). Furthermore, 11.3% (315) of the mutations enhanced *Ras*^{V12}-induced tumor overgrowth but did not exhibit any invasion phenotype (Fig. 1*D*). Finally, 0.7% (23) of the mutations, including 22 lethal and 1 viable, triggered both enhanced tumor overgrowth and metastasis (metastasis-promoting mutations).[6] Two of the metastasis-promoting mutations belong to the same complementation group, *dor*, which has an existing null allele, *dor*^{8} (also see below). Starting on day 8 after egg laying (AEL), *Ras*^{V12} tumors with homozygous *dor* mutation (hereafter referred to as *Ras*^{V12}/*dor*$^{-}$) exhibited enhanced overgrowth when compared with *Ras*^{V12} controls (data not shown). On day 14 AEL, *Ras*^{V12}/*dor*− tumor cells clearly invaded into VNC with a high frequency (75%, n = 24: data not shown). On day 18 AEL, the dramatically overgrown *Ras*^{V12}/*dor*$^{-}$ tumors occupied about one-quarter volume of the larvae body (data not shown) and completely enveloped VNC (Fig. 1*E*, 100%, n = 22; Fig. 1*F*, 100%, n = 29; Fig. 2*G*, 100%, n = 38; Table 1). Occasionally, GFP-labeled tumor cells were also found in the gut and the trachea of the *Ras*^{V12}/*dor*− larvae, indicating secondary tumor formation in distal organs (data not shown). All *Ras*^{V12}/*dor*$^{-}$ larvae died prior to pupation.

TABLE 1
Lysosome dysfunction promotes overgrowth and metastasis of *Ras^{V12}* tumors

Genotype	Tumor overgrowth	Metastasis ratio	*p* value[a]
WT	−	0% ($n > 200$)	NA[b]
Ras^{V12}	+	0% ($n > 200$)	NA[b]
Ras^{V12}/dor^{8}	+++	100% ($n = 38$)	0[c]
Ras^{V12}/Met^{C107}	+++	100% ($n = 22$)	0[c]
Ras^{V12}/Met^{D185}	+++	100% ($n = 29$)	0[c]
Ras^{V12}/dor^{8} + UAS-dor	+	0% ($n = 50$)	1[c]
Ras^{V12} + car^{RNAi}	++	29.8% ($n = 57$)	0.000001[c]
Ras^{V12} + vps16A^{RNAi}	++	34.9% ($n = 43$)	0.000006[c]
Ras^{V12} + 10% phosphate-buffered saline	+	0% ($n = 44$)	NA[b]
Ras^{V12} + chloroquine	++	16.1% ($n = 56$)	0.0014[d]
Ras^{V12} + ethanol	+	0% ($n = 60$)	NA[b]
Ras^{V12} + monensin	++	11.8% ($n = 51$)	0.013[e]

[a] *p* value was calculated using Fisher's exact test.
[b] NA, not applicable.
[c] Compared against *Ras^{V12}*.
[d] Compared against *Ras^{V12}* + 10% phosphate-buffered saline.
[e] Compared against *Ras^{V12}* + monensin. $p < 0.05$ is considered as a significant difference.

To test whether the *dor* mutation alone was sufficient to cause tumorigenesis or metastasis, we generated *dor*$^{-}$ homozygous mutant clones without *Ras^{V12}* in eye tissues using *ey-FLP*. When compared with wild type controls (Fig. 2, *C* and *D*), clones of *dor*− cells displayed no visible growth advantages or morphology defects in either larval or adult stages (Fig. 2, *E* and *F*). However, severe loss of red pigments was observed in the *dor*$^{-}$ clones in the adult eye (Fig. 2*F*), indicating a cell-autonomous pigmentation defect. Taken together, these data indicate that the *dor* mutation itself is not sufficient to induce tumor growth but can collaborate with the oncogene *Ras^{V12}* to trigger tumor overgrowth and metastasis.

dor Behaves as a Metastasis Suppressor—To map an X-linked lethal mutation or to perform complementation tests, we must first rescue the male lethality with a chromosome duplication. Hemizygous *dor* mutant male flies were lethal at the third-instar larvae stage. We examined a collection of chromosome duplications that cover more than 90% of the X chromosome (Bloomington chromosome 1 duplication kit) and successfully rescued the *dor* male lethality by two duplications with an overlap chromosome region from 1A3 to 2B18 (*Dp(1;Y)y^{2}67g19.1*; *Dp(1;f)R*) (Fig. 2*A*). The rescued *dor* mutant males allowed us to perform complementation tests with other lethal metastasis-promoting mutations, which led to the identification of a complementation group containing two alleles (*dor^{C107}* and *dor^{D185}*; Fig. 1, *E* and *F*). Further genetic mapping with strains carrying smaller deficiencies or duplications located *dor* in a chromosome region between 2B1 and 2B5, containing 10 known or predicted genes (Fig. 2*A*). Sequencing of the coding regions of these candidate genes identified two nonsense mutations (T to G and C to T) in the *dor* gene for *dor^{C107}* and *dor^{D185}*, respectively (Fig. 2*B*). Both mutations were expected to result in premature Dor proteins lacking the functionally critical RING-H2 domain (6). The previously existing *dor^{8}* null mutation failed to complement with the new *dor* alleles and exhibited similar phenotypes including third-instar larval lethality in homozygous mutants (19), eye pigmentation defects in clones of *dor*$^{-}$ cells (6), and more importantly, enhanced tumor overgrowth and metastasis in clones of *Ras^{V12}/dor*− cells (Fig. 2*G*). Finally, the wild type *dor* transgene can rescue both the lethality and the tumor phenotypes of all three alleles (Fig. 2, *G–J*; Table 1; and data not shown). Therefore, we conclude that the metastasis-promoting mutations are loss-of-function *dor* alleles and that *dor* encodes a novel metastasis suppressor.

To test whether the effect of *dor* on tumor growth and metastasis is context-dependent, we inactivated *dor* in clones of *dMyc*-overexpressing cells and did not observe tumor overgrowth or metastasis (*dMyc^{over}/dor^{8}*; supplemental Fig. 1*C*). Furthermore, we inactivated *dor* in clones of cells with overexpression of the insulin receptor (*InR*) and observed enhanced tumor overgrowth but not metastasis (*InR^{over}/dor^{8}*; supplemental Fig. 1*D*). These data suggest that the effect of *dor* on tumor growth and metastasis is context-dependent.

Disruption of the Class C VPS Complex Cooperates with Oncogenic Ras^{V12} in Inducing Metastasis—Three genes have been identified to encode different components of the Class C VPS complex in *Drosophila*. Mutations of the other two genes, *car* and *vps16A*, could lead to similar pigmentation and vesicle-trafficking phenotypes as those exhibited in *dor* mutants (6, 7). We thus disrupted *car* or *vps16A* in the same *Ras^{V12}* tumor model to examine their potential effects on metastasis.

We used RNAi to knock down the expression of *car*. Two snap-back *car* cDNA fragments were placed under the transcriptional control of a UAS promoter to form a *car^{RNAi}* transgene. When driven by *Act-Gal4*, the *car^{RNAi}* transgene efficiently impaired the endogenous expression of *car* in one of the transgenic lines. Quantitative real-time reverse transcription-PCR using RNA isolated from the third-instar larvae showed that the *car* mRNA level in *car^{RNAi}* animals was decreased to 37.6% of that in the wild type controls. As a control, *dor* expression was not affected (Fig. 3*A* and data not shown). Transgenic larvae could develop into the pupal stage, but only 4.4% of them ($n = 91$) survived to adult. Consistent with the function of *car* in cargo delivery to pigment granules (6, 20), eye-specific RNAi of *car* induced by *ey-FLP* and *Act>y+>Gal4* resulted in obvious reduction of eye pigments (Fig. 3, *B* and *C*). Knockdown of *car* moderately enhanced the overgrowth of *Ras^{V12}* tumors on day 18 AEL (Fig. 3*F*; Table 1). When compared with the non-invasive *Ras^{V12}* tumors (Fig. 3, *D* and *E*, 0%, $n = 47$), *Ras^{V12}/car^{RNAi}* tumors frequently invaded into the VNC (Fig. 3*G*, 29.8%, $n = 57$; Table 1). Knockdown of *vps16A* in *Ras^{V12}* cells resulted in similar metastatic phenotypes (*Ras^{V12}/vps16A ^{RNAi}*). An established *vps16A^{RNAi}* allele (7) led to tumor invasion toward VNC in *Ras^{V12}* cells (Fig. 3, *H* and *I*, 34.9%, $n = 43$; Table 1). The tumor growth- and metastasis-promoting capabilities of *car^{RNAi}* and *vps16A^{RNAi}* were weaker than that of *dor^{8}*, likely attributing to the fact that the RNAi procedure only reduced but did not eliminate the activity of the genes. Nevertheless, these data clearly indicate a tumor growth and metastasis suppression role of the Class C VPS complex genes in cancer progression.

Impaired Lysosomal Degradation Contributed to Metastatic Behavior—Involvement of the Class C VPS complex in lysosomal delivery suggests that the acquired metastatic capability of *Ras^{V12}* tumor cells may result from defects in lysosomal trafficking. To test this possibility, we examined the lysosomal degradation activity in *Ras^{V12}/dor*$^{-}$ tumor cells with a *GFP-LAMP* transgene. When expressed, the cytoplasmic tail of human

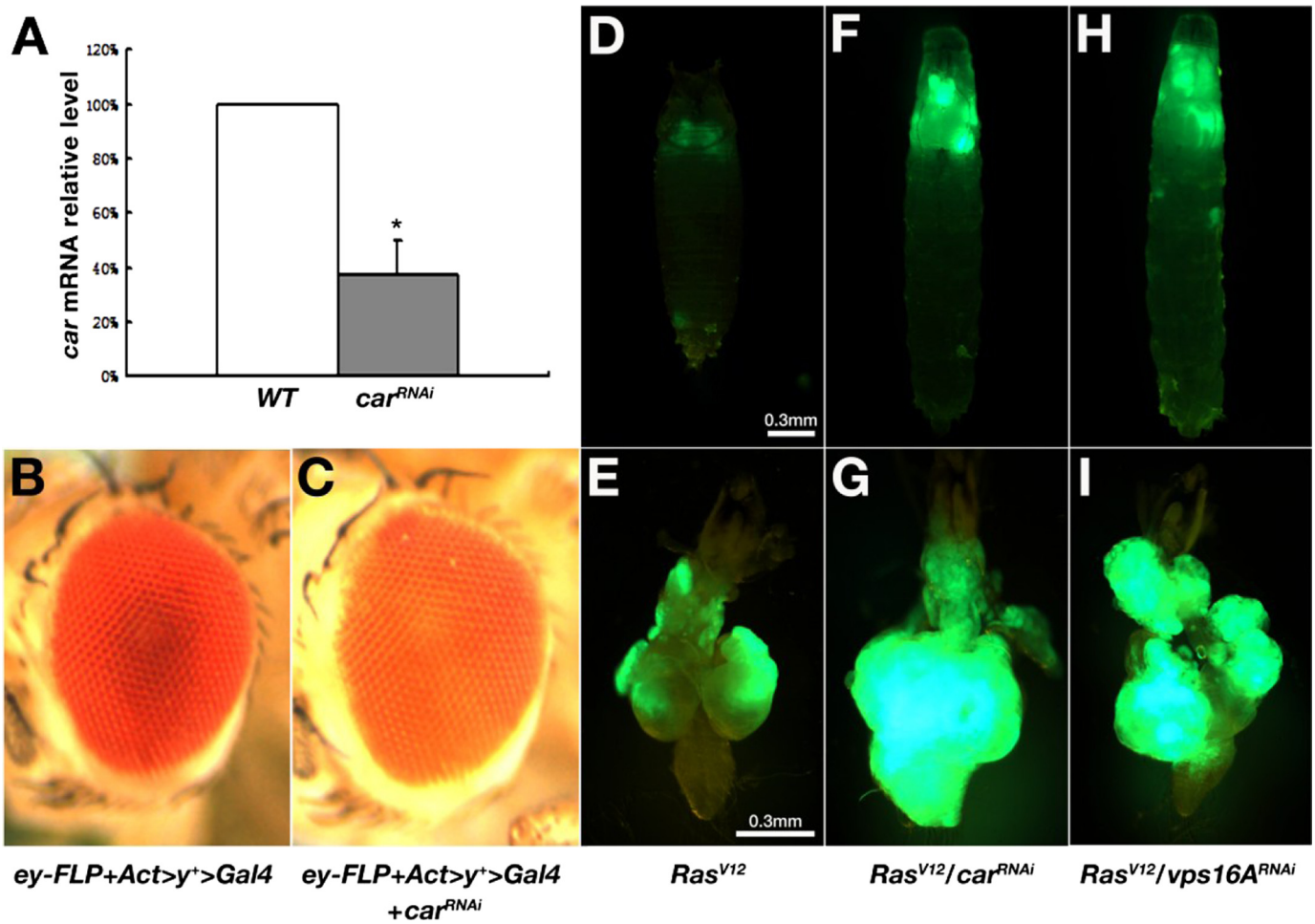

FIGURE 3. **Disruption of the Class C VPS complex promotes tumor growth and metastasis in Ras^{V12} cells.** *A*, quantitative real-time reverse transcription-PCR results indicate that the *car* mRNA level in third-instar larvae was significantly reduced by RNAi. Actin mRNA levels were used as internal controls. *, $p < 0.0001$. *Error bars* indicate S.D. *B* and *C*, micrographs of compound eye from control (*B*) and car^{RNAi} (*C*) flies, indicating the pigmentation defect in the car^{RNAi} eye. *D–I*, larvae/pupae and dissected cephalic complexes from third-instar larvae with indicated genotypes. Both car^{RNAi} and vps16A^{RNAi} cause overgrowth and metastasis of GFP-positive Ras^{V12} cells. *D*, *F*, and *H* are in the same magnification. *E*, *G*, and *I* are in the same magnification.

LAMP1 protein is sufficient to direct the fused GFP to the lysosome for degradation (7). When the transgene is expressed in red fluorescent protein (RFP)-labeled clones of Ras^{V12} cells, only basal level GFP signals were detected, indicating effective lysosomal degradation (Fig. 4, *A–D*). However, massive accumulation of GFP-LAMP proteins were observed in Ras^{V12}/*dor*− tumor cells both in the primary tumors and in the leading edge of invading tumor cells (Fig. 4, *E–H*), revealing impaired lysosomal degradation.

We also blocked lysosomal degradation in Ras^{V12} tumors by chloroquine or monensin treatment. These two traditional antimalarial drugs have been reported to be able to inhibit lysosomal degradation by raising intralysosomal pH (21, 22). Ras^{V12} larvae were bred on chloroquine- or monensin-containing medium to score the tumor phenotypes. The treatment of either chloroquine or monensin clearly promoted metastasis. On day 18 AEL, 16.1% of the chloroquine-treated Ras^{V12} tumors have prominently invaded into the VNC, although the overgrowth was not notably enhanced (Fig. 4*J*, $n = 56$; Table 1). In contrast, the invasive behavior was never observed in control tumors fed with solvent only medium (Fig. 4*I*, $n = 44$; Table 1). Monensin treatment resulted in similar phenotypes. 11.8% of the monensin-treated Ras^{V12} animals developed VNC invasion (Fig. 4*L*, $n = 51$; Table 1), in comparison with no invasion in the control group (Fig. 4*K*, $n = 60$; Table 1). Taken together, these data indicate that lysosomal degradation impairment can cooperate with Ras^{V12} to promote tumor progress and metastasis.

Autophagy, a process involving degradation of cellular components by fusion with the lysosome, has been indicated to play important roles in cancer development (23, 24). However, data suggest that the process could have opposing roles in tumorigenesis (23, 24). *beclin1* (*atg6*) and *UVRAG* (*vps38*), two components of the autophagy pathway, have been identified as tumor suppressors (25–27). On the other hand, autophagy has also been implicated for a tumor-promoting role by its contribution to the survival of tumor cells under stress conditions (28). Because the Class C VPS complex is essential in both the endosome-lysosome and the autophagosome-lysosome fusion processes (7, 29, 30), we thus examined whether disruption of the autophagy pathway could contribute to enhanced tumor overgrowth and metastasis. Because *atg5* and *atg7* are required for autophagy in mammals and *Drosophila* (31, 32), we used the established *atg5* or *atg7* RNAi allele (31) to knock down the activity of autophagy in clones of Ras^{V12} cells.

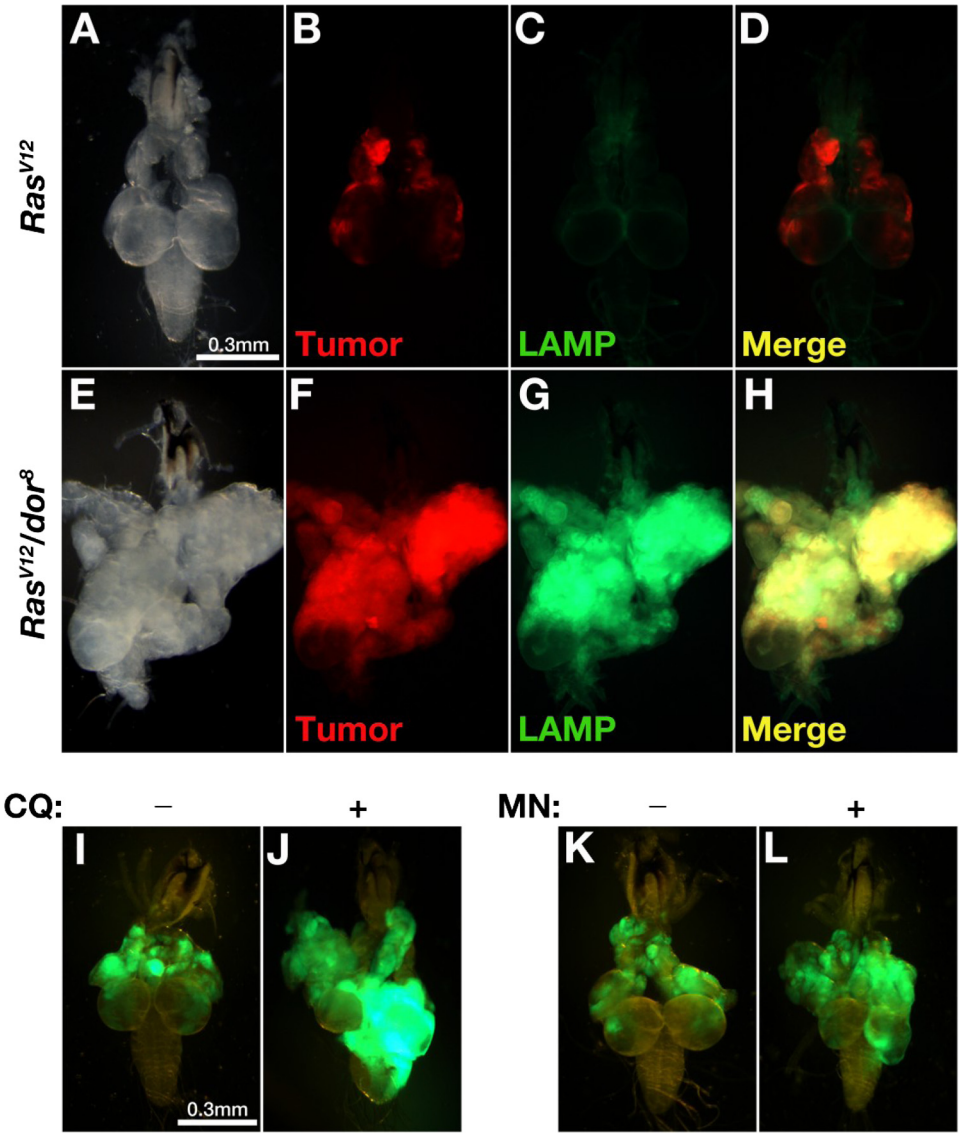

FIGURE 4. **Impaired lysosomal degradation contributes to metastasis.** Dissected cephalic complexes from third-instar larvae are shown. *A–H*, RFP was used for labeling tumor clones to distinguish them from the green signal of the GFP-LAMP fusion protein. *I–L*, Ras^{V12} tumor cells were labeled by GFP. In Ras^{V12} tumors (*A–D*), GFP-LAMP fusion proteins were presumably targeted to lysosomes and efficiently degraded. With additional *dor*^{8} mutation, the lysosomal degradation of GFP-LAMP proteins was blocked inside tumor tissues with invasive potential (*E–H*). Inhibition of lysosomal degradation by feeding chloroquine (*CQ*) (*J*) or monensin (*MN*) (*L*) induced VNC invasion of Ras^{V12} tumor clones (*green*) when compared with the control samples (*I* and *K*).

Neither enhanced tumor overgrowth nor metastasis was observed (data not shown). Furthermore, in *Drosophila*, activation of the JNK signaling pathway has been shown to promote the overgrowth and the metastasis of Ras^{V12} cells with disrupted cell polarity (Ras^{V12}/*scrib*$^{-}$) (33–35). We also disrupted the JNK pathway by expressing a dominant negative form of the *Drosophila* JNK gene (*bsk*^{DN}) in the Ras^{V12}/*dor*− tumor cells. We found that both enhanced tumor overgrowth and metastasis of the Ras^{V12}/*dor*$^{-}$ tumors were almost completely suppressed (supplemental Fig. 1*E*). Together, these data suggest that activation of the JNK signaling, rather than disruption of autophagy, is likely the cause of the phenotypes observed in the Ras^{V12}/*dor*− tumors.

DISCUSSION

Deregulation of lysosome functions is linked to many pathological conditions including cancer (36). Dor/Vps18 is one of the essential players in the lysosomal delivery pathway, and its functions have been conserved from yeast to mammals (6, 14, 37, 38). Our study shows that *dor* functions as a suppressor of tumor growth and metastasis. Although inactivation of *dor* did not trigger tumorigenesis by itself, it promotes both tumor growth and metastasis in cooperation with oncogenic *Ras*. Consistent with disruption of the Class C VPS complex, inactivation of either of the two other components of the complex, *car* and *vps16A*, resulted in similar tumor growth and metastasis phenotypes. These data indicate that components of the Class C VPS complex behave as metastasis suppressors.

Our data showed that administration of antimalarial drugs, chloroquine or monensin, has a profound effect on promoting tumor progression and metastasis of cells expressing oncogenic *Ras*. Chloroquine treatment has been reported to have a suppression effect on *Myc*-induced lymphoma in mice (39). On the other hand, recent studies of chloroquine and quinacrine, another antimalarial drug, have shown promotion of tumor development in rats (40). Perhaps the effect of lysosomal degradation blockage on tumor development and progression is context-dependent. Indeed, we observed that the effect of *dor* mutations on tumor overgrowth and metastasis is Ras^{V12}-dependent. The *dor* mutation has no effect on *dMyc*-overexpressing cells and only enhances growth of the *InR*-overexpressing cells. Our study, taken together with the previous reports, argues for further careful examination of the effect of antimalarial drugs on tumor development and progression.

Autophagy has been indicated to play important roles in cancer development. However, disruption of autophagy is unlikely to be the major cause of the phenotypes that we observed in the Ras^{V12}/*dor*$^{-}$ tumors because inactivation of either of two key components of the autophagy pathway, *atg5* and *atg7*, did not enhance tumor overgrowth or metastasis of the Ras^{V12} cells. On the other hand, disruption of the JNK signaling in the Ras^{V12}/*dor*− tumors blocked both enhanced tumor overgrowth and metastasis. This is consistent with the previous observation that activation of the JNK signaling plays an essential role in tumor growth and progression (33–35).

Cellular homeostasis is tightly controlled in living cells. Normal cells have the ability to modulate the rates of molecular synthesis and degradation in response to different developmental and physiological stimuli. Impaired lysosomal degradation has been detected in cancer and other pathological conditions and is believed to be able to increase the cell mass (41–43). Consistent with this notion, *Ras^{V12}/dor^{-}* tumors exhibited a dramatic overgrowth phenotype. In those studies, however, the role of lysosomal degradation in tumor metastasis is less obvious. Future study is needed to explore whether any processes or signaling events that promote metastasis are affected by lysosomal degradation. Analysis of the downstream events will help to understand how impaired lysosomal degradation contributes to malignant transformation and may indicate a novel direction for therapeutic intervention against metastasis.

Acknowledgments—We sincerely thank Helmut Krämer (UT Southwestern Medical Center), Thomas P. Neufeld (University of Minnesota), the Kyoto Stock Center, and the Bloomington Stock Center for providing various fly strains, Fei Gu, Sheng Shi, and Beibei Song for technical assistance, and Beibei Ying, Kejing Deng, Rener Xu, Wufan Tao, Ling Sun, Zhisheng Ye, Chi Zhang, and other members of the Institute of Developmental Biology and Molecular Medicine for discussions.

REFERENCES

1. Rochefort, H., Capony, F., and Garcia, M. (1990) *Cancer Metastasis Rev.* **9,** 321–331
2. Hirano, T., Manabe, T., and Takeuchi, S. (1993) *Cancer Lett.* **70,** 41–44
3. Brouillet, J. P., Dufour, F., Lemamy, G., Garcia, M., Schlup, N., Grenier, J., Mani, J. C., and Rochefort, H. (1997) *Cancer* **79,** 2132–2136
4. Banta, L. M., Robinson, J. S., Klionsky, D. J., and Emr, S. D. (1988) *J. Cell Biol.* **107,** 1369–1383
5. Preston, R. A., Manolson, M. F., Becherer, K., Weidenhammer, E., Kirkpatrick, D., Wright, R., and Jones, E. W. (1991) *Mol. Cell. Biol.* **11,** 5801–5812
6. Sevrioukov, E. A., He, J. P., Moghrabi, N., Sunio, A., and Krämer, H. (1999) *Mol. Cell* **4,** 479–486
7. Pulipparacharuvil, S., Akbar, M. A., Ray, S., Sevrioukov, E. A., Haberman, A. S., Rohrer, J., and Krämer, H. (2005) *J. Cell Sci.* **118,** 3663–3673
8. Lloyd, V., Ramaswami, M., and Krämer, H. (1998) *Trends Cell Biol.* **8,** 257–259
9. Kim, B. Y., Krämer, H., Yamamoto, A., Kominami, E., Kohsaka, S., and Akazawa, C. (2001) *J. Biol. Chem.* **276,** 29393–29402
10. Huizing, M., Didier, A., Walenta, J., Anikster, Y., Gahl, W. A., and Krämer, H. (2001) *Gene* **264,** 241–247
11. Suzuki, T., Oiso, N., Gautam, R., Novak, E. K., Panthier, J. J., Suprabha, P. G., Vida, T., Swank, R. T., and Spritz, R. A. (2003) *Proc. Natl. Acad. Sci. U.S.A.* **100,** 1146–1150
12. Poupon, V., Stewart, A., Gray, S. R., Piper, R. C., and Luzio, J. P. (2003) *Mol. Biol. Cell* **14,** 4015–4027
13. Sadler, K. C., Amsterdam, A., Soroka, C., Boyer, J., and Hopkins, N. (2005) *Development* **132,** 3561–3572
14. Maldonado, E., Hernandez, F., Lozano, C., Castro, M. E., and Navarro, R. E. (2006) *Pigment Cell Res.* **19,** 315–326
15. Yu, J. F., Fukamachi, S., Mitani, H., Hori, H., and Kanamori, A. (2006) *Pigment Cell Res.* **19,** 628–634
16. Pagliarini, R. A., and Xu, T. (2003) *Science* **302,** 1227–1231
17. Lee, Y. S., and Carthew, R. W. (2003) *Methods* **30,** 322–329
18. Spradling, A. C., and Rubin, G. M. (1982) *Science* **218,** 341–347
19. Shestopal, S. A., Makunin, I. V., Belyaeva, E. S., Ashburner, M., and Zhimulev, I. F. (1997) *Mol. Gen. Genet.* **253,** 642–648
20. Sriram, V., Krishnan, K. S., and Mayor, S. (2003) *J. Cell Biol.* **161,** 593–607
21. Seglen, P. O., Grinde, B., and Solheim, A. E. (1979) *Eur. J. Biochem.* **95,** 215–225
22. Grinde, B. (1983) *Exp. Cell Res.* **149,** 27–35
23. Kondo, Y., Kanzawa, T., Sawaya, R., and Kondo, S. (2005) *Nat. Rev. Cancer* **5,** 726–734
24. Mathew, R., Karantza-Wadsworth, V., and White, E. (2007) *Nat. Rev. Cancer* **7,** 961–967
25. Aita, V. M., Liang, X. H., Murty, V. V., Pincus, D. L., Yu, W., Cayanis, E., Kalachikov, S., Gilliam, T. C., and Levine, B. (1999) *Genomics* **59,** 59–65
26. Liang, X. H., Jackson, S., Seaman, M., Brown, K., Kempkes, B., Hibshoosh, H., and Levine, B. (1999) *Nature* **402,** 672–676
27. Liang, C., Feng, P., Ku, B., Dotan, I., Canaani, D., Oh, B. H., and Jung, J. U. (2006) *Nat. Cell Biol.* **8,** 688–699
28. Degenhardt, K., Mathew, R., Beaudoin, B., Bray, K., Anderson, D., Chen, G., Mukherjee, C., Shi, Y., Gélinas, C., Fan, Y., Nelson, D. A., Jin, S., and White, E. (2006) *Cancer Cell* **10,** 51–64
29. Liang, C., Lee, J. S., Inn, K. S., Gack, M. U., Li, Q., Roberts, E. A., Vergne, I., Deretic, V., Feng, P., Akazawa, C., and Jung, J. U. (2008) *Nat. Cell Biol.* **10,** 776–787
30. Lindmo, K., Simonsen, A., Brech, A., Finley, K., Rusten, T. E., and Stenmark, H. (2006) *Exp. Cell Res.* **312,** 2018–2027
31. Scott, R. C., Schuldiner, O., and Neufeld, T. P. (2004) *Dev. Cell* **7,** 167–178
32. Jaeger, P. A., and Wyss-Coray, T. (2009) *Mol. Neurodegener.* **4,** 16
33. Wu, M., Pastor-Pareja, J. C., and Xu, T. (2010) *Nature* **463,** 545–548
34. Igaki, T., Pastor-Pareja, J. C., Aonuma, H., Miura, M., and Xu, T. (2009) *Dev. Cell* **16,** 458–465
35. Igaki, T., Pagliarini, R. A., and Xu, T. (2006) *Curr. Biol.* **16,** 1139–1146
36. Polo, S., Pece, S., and Di Fiore, P. P. (2004) *Curr. Opin. Cell Biol.* **16,** 156–161
37. Yogosawa, S., Hatakeyama, S., Nakayama, K. I., Miyoshi, H., Kohsaka, S., and Akazawa, C. (2005) *J. Biol. Chem.* **280,** 41619–41627
38. Rieder, S. E., and Emr, S. D. (1997) *Mol. Biol. Cell* **8,** 2307–2327
39. Amaravadi, R. K., Yu, D., Lum, J. J., Bui, T., Christophorou, M. A., Evan, G. I., Thomas-Tikhonenko, A., and Thompson, C. B. (2007) *J. Clin. Invest.* **117,** 326–336
40. Dutta, P., Karmali, R., Pinto, J. T., and Rivlin, R. S. (1994) *Cancer Lett.* **76,** 113–119
41. Kisen, G. O., Tessitore, L., Costelli, P., Gordon, P. B., Schwarze, P. E., Baccino, F. M., and Seglen, P. O. (1993) *Carcinogenesis* **14,** 2501–2505
42. Bradley, M. O. (1977) *J. Biol. Chem.* **252,** 5310–5315
43. Tessitore, L., Bonelli, G., Cecchini, G., Autelli, R., Amenta, J. S., and Baccino, F. M. (1988) *Biochem. J.* **251,** 483–490